R. & M. No. 3092
(19,057)
A.R.C. Technical Report

MINISTRY OF SUPPLY

AERONAUTICAL RESEARCH COUNCIL
REPORTS AND MEMORANDA

Observations of the Flow Past a Two-Dimensional 4 per cent Thick Biconvex Aerofoil at High Subsonic Speeds

By

B. D. Henshall, B.Sc., Ph.D.,
and R. F. Cash, A.F.R.Ae.S., of the Aerodynamics Division, N.P.L.

LONDON: HER MAJESTY'S STATIONERY OFFICE
1958
PRICE 6*s.* 6*d.* NET

Observations of the Flow Past a Two-Dimensional 4 per cent Thick Biconvex Aerofoil at High Subsonic Speeds

By

B. D. Henshall, B.Sc., Ph.D.,
and R. F. Cash, A.F.R.Ae.S., of the Aerodynamics Division, N.P.L.

Reports and Memoranda No. 3092*
February, 1957

Summary.—Flow photographs and detailed pressure distributions for a 4 per cent thick circular-arc biconvex aerofoil at high subsonic speeds and high incidences have been analysed and the divergence boundary (defining the onset of separation effects) for the aerofoil determined. Emphasis was placed on the transition from leading-edge to shock-induced separation as the free-stream Mach number was raised at a fixed incidence.

1. *Introduction.*—Recent tests in the 36-in. × 14-in. High-Speed Wind Tunnel of the National Physical Laboratory have included the investigation of the flow past a 4 per cent thick circular-arc biconvex aerofoil over wide ranges of incidence and at speeds from low subsonic ($M_0 = 0{\cdot}40$) to moderate supersonic ($M_0 = 1{\cdot}60$).

In a previous report[1] an analysis was made of the occurrence of leading-edge flow separation at low speeds ($M_0 = 0{\cdot}40$ to $0{\cdot}70$), and the present report describes studies made of the transition from leading-edge to shock-induced separation as the free-stream Mach number was raised at a fixed incidence. Both series of tests were made with solid-wall subsonic liners fitted in the 36-in. × 14-in. High-Speed Wind Tunnel and no corrections have been made for tunnel-wall interference effects (in a subsequent paper a description will be given of similar tests made using slotted-wall transonic liners).

The Reynolds numbers of the current tests varied from $2{\cdot}6 \times 10^6$ at $M_0 = 0{\cdot}60$ to $3{\cdot}3 \times 10^6$ at $M_0 = 0{\cdot}90$ based on the aerofoil chord of 9 in.; the boundary layers were naturally turbulent and were not subjected to artificial transition methods (*see* Ref. 1 for further details).

2. *Experimental Data.*—The detailed pressure distributions obtained during the experiments are presented in Tables 1 to 5. These results were plotted and integrated to give the normal-force coefficients and the pitching-moment coefficients. Curves of normal-force coefficient C_N against free-stream Mach number M_0 for various incidences α are given in Fig. 1; curves of pitching-moment coefficient C_m about $0{\cdot}25c$ against M_0 for various α are given in Fig. 2 and Fig. 3 is a cross-plot of C_m against C_N from Figs. 1 and 2. Specimen series of pressure distributions for increasing free-stream Mach number at constant incidences of 4 deg and 5 deg are given in Figs. 4 and 6 respectively, and the corresponding schlieren photographs appear as Figs. 5 and 7. As the incidence of the aerofoil is increased in intervals of 1 deg the transition from leading-edge to shock-induced separation, as the free-stream Mach number is raised, becomes very abrupt. Fig. 8 presents schlieren photographs of this transition at angles of incidence of 6, 7, 8 and 9 deg. Detailed pressure distributions before and after the transition for the case $\alpha = 6$ deg are given in Fig. 9.

* Published with permission of the Director, National Physical Laboratory.

3. *Analysis of Results.*—During recent years the problems of shock-induced boundary-layer separations have been extensively studied at the N.P.L.[2, 3]. In particular, a qualitative discussion of the occurrence and development of boundary-layer separations at high incidences and high speeds has been given by Pearcey[4], where the transition from leading-edge to shock-induced separation as the free-stream Mach number is raised at fixed incidence, is discussed in some detail. One of the most important results of this work has been the general adoption of ' divergence ' of trailing-edge pressure from its normal smooth variation as the prime indicator of the onset of the effects of separation. The N.P.L. has proposed the use of this term ' divergence ' which is synonymous with ' the onset of the effects of separation ' and the use of ' separation ' in its literal sense. This distinction between the first occurrence of a separation bubble somewhere on the surface of the aerofoil and the advent of the effects of separation on the various flow parameters, for example, C_N or $(p/H_0)_{TE}$, has proved particularly valuable for aerofoils at high incidences.

At low incidences divergence occurs almost immediately after separation[2]. However, at high incidences there is an appreciable delay between separation and divergence. The separation bubble at first grows slowly in chordwise extent until, at a certain stage, it expands abruptly or ' bursts '; divergence appears to coincide with this occurrence.

In addition to the results presented above, detailed surveys were made of the variation of trailing-edge pressure with Mach number for several constant incidences. These results are presented in Fig. 10 in the form of curves of (p_{TE}/H_0) against (p_0/H_0). Furthermore, Fig. 11 repeats this data with the more convenient ordinate $(p_0 - p_{TE})/H_0$ instead of (p_{TE}/H_0). The divergence of the parameter $(p_0 - p_{TE})/H_0$, as the free-stream Mach number M_0 is increased at constant incidence α, is particularly marked. At the higher incidences, however, a very sudden change from the normal smooth variation occurs in the opposite sense to divergence. This coincides with the change from a flow with a leading-edge separation to an attached flow with a shock wave and the pitching-moment curves (Fig. 2) also show corresponding sharp ' nose-up ' pitching-moment changes. Fig. 11c shows in a schematic form the expected variation, if separation effects were absent, of the parameter $(p_0 - p_{TE})/H_0$ with free-stream Mach number for various constant incidences. The curve for $\alpha = 2$ deg shows the usual divergence due to the onset of the effects of shock-induced separation. Before this divergence occurs the trailing-edge is unaffected by separation on the upper surface of the aerofoil. However, for $\alpha = 4$ deg the effects of leading-edge separation are present from low free-stream Mach numbers and the parameter $(p_0 - p_{TE})/H_0$ varies smoothly but in the opposite sense to the curve for $\alpha = 2$ deg. This may be regarded as a slow divergence from the curve which would be expected if separation effects were absent. When the flow attaches at the leading edge there is an abrupt transition back to the curve for no separation effects and subsequently trailing-edge divergence from shock-induced separation occurs. For angles of incidence greater than 4 deg the observed curve does not return to the anticipated one for no separation effects when flow reattachment occurs. From curves such as Figs. 10 and 11 and the corresponding cross-plots of (p_{TE}/H_0) and $(p_0 - p_{TE}/H_0)$ against incidence α for several constant M_0 (or p_0/H_0)*, a locus of points (α_D, M) for the divergence of trailing-edge pressure may be drawn. Fig. 12 is the divergence boundary of the two-dimensional 4 per cent thick biconvex aerofoil in the subsonic liners of the 36-in. × 14-in. High-Speed Wind Tunnel at N.P.L. (Note that the experimental data have not been corrected for blockage effects.)

Divergence boundaries for finite wings show precisely the same qualitative trends as Fig. 12. Moreover, flight-determined ' boundaries ' for the occurrence of buffeting and ' pitch-up ' instability (phenomena known to be associated with separation), again show qualitative agreement with curves such as Fig. 12. Each discrete regime of flow is labelled in Fig. 12 and the (α, M) conditions are shown for the transition from unseparated flow to flow with the effects of separation, which may be of the leading-edge or shock-induced type. The locus of points where shock waves were first observed to occur is also plotted in Fig. 12 and it may be noted that in an appreciable region a separation bubble was present but divergence had not occurred. Several series of Schlieren photographs, which are applicable to Fig. 12, are given in this report and elsewhere[1]. Finally, let us consider Fig. 13 for a specific illustration of the general flow development about

* Not reproduced.

this 4 per cent biconvex aerofoil as the Mach number is raised at a fixed incidence of 5 deg. In Fig. 13 the contributions of the separate surfaces to the total C_N on the aerofoil are shown, and from these results the following description of the flow development as the Mach number is raised may be built up. The various regimes of flow are denoted by O, A, B, C, . . . :

- O → A Flow with leading-edge separation. Lower surface unaffected by effects of separation.
- A → B Reattachment of flow at leading-edge. Local shock-induced separation present with almost immediate reattachment.
- B → C Normal backward progression of upper-surface shock wave with very small separation bubble at foot of shock.
- C → D Shock-induced separation growing gradually more severe but not affecting the lift on the lower surface. At point D the separation bubble has reached the trailing edge.
- D → E Rapid growth of shock-induced separated region, slowing up movement of shock on upper surface and affecting the lift on the lower surface.
- E → F Reacceleration of upper-surface shock.
- F → G Shock reaches trailing edge.

4. *Conclusions.*—The divergence boundary for a two-dimensional 4 per cent thick biconvex aerofoil has been determined in the 36-in. × 14-in. High-Speed Wind Tunnel at the N.P.L. The most noticeable feature of the tests on this aerofoil was the very abrupt flow attachment at high incidences when the Mach number was slowly raised above $M_0 = 0{\cdot}70$. In an appreciable region of the (α, M) diagram a separation bubble was present on the upper surface of the aerofoil but the onset of the effects of separation (that is, by definition, divergence) had not occurred.

Acknowledgements.—Mr. P. J. Peggs assisted in the experimental work, and Mrs. N. A. North helped in the data reduction.

NOTATION

M_0	Free-stream Mach number (uncorrected)
H_0	Stagnation pressure
p	Local static pressure
C_N	Normal-force coefficient (uncorrected)
C_m	Pitching moment (about 0·25 chord) coefficient (uncorrected)
c	Aerofoil chord
α	Aerofoil incidence (uncorrected)

Suffices

$_0$	Value of a quantity in the free stream
$_{TE}$	Value of a quantity at the trailing edge of the aerofoil
$_D$	Value of a variable (i.e., α or M) at which the variation of a quantity (e.g., p_{TE}/H_0) diverges due to separation.

REFERENCES

No.	*Author*	*Title, etc.*
1	B. D. Henshall and R. F. Cash	An experimental investigation of leading-edge flow separation from a 4 per cent thick two-dimensional biconvex aerofoil. R. & M. 3091. February, 1957.
2	D. W. Holder, H. H. Pearcey, G. E. Gadd (all of N.P.L.) and J. Seddon (R.A.E.).	The interaction between shock waves and boundary layers (with a note on 'The effects of the interaction on the performance of supersonic intakes'). C.P. 180. February, 1954.
3	H. H. Pearcey	Some effects of shock-induced separation of turbulent boundary layers in transonic flow past aerofoils (Paper No. 9 presented at the Symposium on Boundary-Layer Effects in Aerodynamics at N.P.L., 31st March to 2nd April, 1955). A.R.C. 17,681. June, 1955.
4	H. H. Pearcey	The occurrence and development of boundary-layer separations at high incidences and high speeds. A.R.C. 17,901. 30th September, 1955.

TABLE 1

$\alpha = 2$ deg

Experimental Results : Detailed Pressure Distributions for 4 per cent thick Biconvex Aerofoil

	Hole position x/c (per cent)	Values of p/H_0								
		$M_0 =$ 0·60	$M_0 =$ 0·70	$M_0 =$ 0·731	$M_0 =$ 0·771	$M_0 =$ 0·820	$M_0 =$ 0·850	$M_0 =$ 0·871	$M_0 =$ 0·886	$M_0 =$ 0·894
UPPER SURFACE	1	0·584	0·436	0·344	0·204	0·225	0·223	0·294	0·289	0·330
	2	0·586	0·450	0·397	0·267	0·277	0·312	0·336	0·366	0·371
	5	0·636	0·521	0·473	0·352	0·351	0·376	0·400	0·417	0·421
	10	0·739	0·639	0·565	0·577	0·391	0·414	0·433	0·452	0·456
	16	0·740	0·657	0·623	0·598	0·410	0·423	0·444	0·454	0·463
	22	0·739	0·655	0·624	0·587	0·405	0·416	0·428	0·437	0·442
	28	0·737	0·652	0·623	0·580	0·402	0·411	0·419	0·429	0·430
	34	0·740	0·657	0·627	0·585	0·392	0·397	0·429	0·440	0·444
	40	0·741	0·659	0·630	0·587	0·396	0·397	0·401	0·409	0·421
	46	0·741	0·658	0·628	0·585	0·535	0·411	0·407	0·420	0·420
	52	0·744	0·661	0·632	0·590	0·569	0·395	0·410	0·421	0·423
	58	0·747	0·667	0·639	0·598	0·573	0·392	0·406	0·411	0·404
	64	0·751	0·673	0·645	0·607	0·576	0·401	0·399	0·401	0·399
	70	0·753	0·676	0·651	0·612	0·578	0·394	0·391	0·391	0·391
	76	0·760	0·686	0·660	0·625	0·588	0·550	0·379	0·379	0·380
	82	0·767	0·696	0·671	0·638	0·603	0·569	0·395	0·364	0·364
	88	0·777	0·709	0·685	0·656	0·622	0·596	0·535	0·435	0·359
	94	0·787	0·724	0·704	0·676	0·645	0·615	0·567	0·536	0·348
	97	0·799	0·739	0·718	0·696	0·667	0·629	0·574	0·547	0·347
	100	0·803	0·748	0·725	0·705	0·679	0·634	0·585	0·561	0·430
LOWER SURFACE	0·5	0·930	0·908	0·867	0·895	0·882	0·852	0·835	0·810	0·809
	1·5	0·899	0·869	0·852	0·850	0·836	0·799	0·790	0·762	0·767
	3	0·871	0·833	0·824	0·810	0·793	0·770	0·750	0·733	0·727
	6	0·846	0·801	0·789	0·773	0·752	0·729	0·709	0·693	0·687
	10	0·828	0·778	0·765	0·745	0·723	0·699	0·677	0·663	0·655
	18	0·807	0·749	0·733	0·710	0·684	0·659	0·635	0·616	0·612
	26	0·794	0·731	0·713	0·687	0·657	0·630	0·603	0·583	0·577
	34	0·784	0·717	0·698	0·667	0·632	0·606	0·569	0·557	0·537
	42	0·777	0·712	0·692	0·663	0·627	0·592	0·564	0·545	0·535
	50	0·776	0·706	0·682	0·655	0·618	0·582	0·550	0·526	0·509
	58	0·773	0·702	0·682	0·650	0·611	0·579	0·534	0·504	0·494
	66	0·772	0·700	0·678	0·646	0·606	0·571	0·519	0·491	0·475
	73	0·776	0·704	0·681	0·651	0·613	0·576	0·530	0·486	0·461
	79	0·776	0·705	0·685	0·652	0·614	0·581	0·532	0·474	0·449
	85	0·778	0·708	0·689	0·657	0·620	0·583	0·544	0·464	0·436
	91	0·783	0·715	0·699	0·665	0·629	0·603	0·556	0·532	0·425
	97	0·796	0·734	—	0·690	0·660	—	0·577	—	0·424
	100	0·803	0·748	0·725	0·705	0·679	0·634	0·585	0·561	0·430

TABLE 2

$\alpha = 3$ deg

Experimental Results : Detailed Pressure Distributions for 4 per cent thick Biconvex Aerofoil

	Hole position x/c (per cent)	Values of p/H_0							
		$M_0 =$ 0·60	$M_0 =$ 0·70	$M_0 =$ 0·717	$M_0 =$ 0·725	$M_0 =$ 0·734	$M_0 =$ 0·792	$M_0 =$ 0·865	$M_0 =$ 0·880
UPPER SURFACE	1	0·574	0·421	0·336	0·337	0·122	0·139	0·211	0·238
	2	0·570	0·414	0·376	0·379	0·190	0·207	0·304	0·321
	5	0·568	0·422	0·384	0·366	0·287	0·287	0·360	0·364
	10	0·598	0·468	0·446	0·444	0·377	0·332	0·397	0·412
	16	0·684	0·547	0·526	0·530	0·602	0·355	0·404	0·417
	22	0·727	0·614	0·599	0·587	0·613	0·357	0·398	0·408
	28	0·732	0·639	0·619	0·611	0·606	0·360	0·394	0·402
	34	0·734	0·647	0·626	0·621	0·611	0·356	0·378	0·385
	40	0·735	0·650	0·631	0·624	0·613	0·362	0·382	0·386
	46	0·735	0·651	0·633	0·627	0·613	0·510	0·391	0·397
	52	0·738	0·655	0·637	0·632	0·619	0·557	0·375	0·382
	58	0·742	0·660	0·644	0·637	0·627	0·586	0·368	0·373
	64	0·746	0·667	0·651	0·645	0·634	0·600	0·379	0·384
	70	0·749	0·672	0·657	0·651	0·639	0·608	0·372	0·373
	76	0·757	0·683	0·667	0·662	0·652	0·615	0·362	0·365
	82	0·764	0·692	0·678	0·673	0·663	0·627	0·351	0·352
	88	0·774	0·705	0·692	0·687	0·680	0·643	0·431	0·344
	94	0·785	0·720	0·708	0·703	0·698	0·645	0·517	0·337
	97	0·795	0·733	0·720	0·717	0·716	0·646	0·526	0·342
	100	0·802	0·741	0·723	0·721	0·722	0·656	0·537	0·425
LOWER SURFACE	0·5	0·955	0·940	0·937	0·936	0·937	0·923	0·852	0·837
	1·5	0·923	0·900	0·885	0·895	0·894	0·876	0·795	0·784
	3	0·892	0·861	0·856	0·854	0·852	0·833	0·768	0·753
	6	0·865	0·826	0·819	0·817	0·814	0·792	0·725	0·711
	10	0·845	0·800	0·792	0·789	0·786	0·760	0·694	0·679
	18	0·820	0·768	0·759	0·755	0·751	0·721	0·649	0·634
	26	0·804	0·746	0·736	0·732	0·726	0·694	0·615	0·599
	34	0·793	0·730	0·718	0·714	0·709	0·678	0·584	0·566
	42	0·789	0·723	0·712	0·707	0·702	0·663	0·572	0·553
	50	0·783	0·716	0·704	0·699	0·694	0·653	0·555	0·533
	58	0·779	0·710	0·699	0·693	0·687	0·644	0·540	0·508
	66	0·776	0·706	0·693	0·687	0·682	0·636	0·516	0·497
	73	0·779	0·708	0·696	0·691	0·686	0·642	0·519	0·479
	79	0·778	0·708	0·696	0·690	0·685	0·641	0·513	0·468
	85	0·779	0·711	0·698	0·693	0·688	0·646	0·505	0·451
	91	0·784	0·716	0·706	0·699	0·695	0·653	0·525	0·441
	97	0·792	0·725	0·713	0·708	0·705	0·664	—	—
	100	0·802	0·741	0·723	0·721	0·722	0·656	0·537	0·425

TABLE 3

$\alpha = 4$ deg

Experimental Results : Detailed Pressure Distributions for 4 per cent thick Biconvex Aerofoil

	Hole position x/c (per cent)	Values of p/H_0								
		$M_0 =$ 0·60	$M_0 =$ 0·723	$M_0 =$ 0·728	$M_0 =$ 0·740	$M_0 =$ 0·771	$M_0 =$ 0·790	$M_0 =$ 0·809	$M_0 =$ 0·840	$M_0 =$ 0·874
UPPER SURFACE	1	0·570	0·327	0·096	0·097	0·105	0·115	0·144	0·160	0·190
	2	0·569	0·311	0·128	0·136	0·144	0·178	0·206	0·250	0·276
	5	0·567	0·320	0·231	0·234	0·247	0·258	0·285	0·315	0·335
	10	0·565	0·363	0·293	0·290	0·296	0·305	0·324	0·352	0·371
	16	0·585	0·445	0·332	0·321	0·331	0·325	0·345	0·364	0·381
	22	0·633	0·492	0·549	0·429	0·326	0·329	0·344	0·363	0·375
	28	0·681	0·554	0·601	0·542	0·332	0·334	0·346	0·364	0·373
	34	0·713	0·577	0·617	0·589	0·331	0·331	0·341	0·352	0·360
	40	0·727	0·600	0·619	0·610	0·380	0·334	0·340	0·357	0·367
	46	0·734	0·615	0·615	0·609	0·528	0·323	0·330	0·344	0·367
	52	0·738	0·624	0·618	0·611	0·551	0·473	0·327	0·336	0·342
	58	0·741	0·634	0·625	0·614	0·583	0·472	0·345	0·343	0·350
	64	0·747	0·643	0·633	0·620	0·600	0·486	0·491	0·335	0·345
	70	0·750	0·651	0·638	0·623	0·613	0·531	0·506	0·334	0·339
	76	0·757	0·661	0·650	0·636	0·612	0·550	0·512	0·329	0·338
	82	0·764	0·671	0·662	0·649	0·632	0·563	0·523	0·348	0·337
	88	0·772	0·684	0·678	0·667	0·643	0·586	0·534	0·439	0·329
	94	0·782	0·698	0·696	0·685	0·660	0·614	0·555	0·503	0·320
	97	0·790	0·706	0·712	0·702	0·679	0·614	0·558	0·512	0·340
	100	0·796	0·713	0·726	0·715	0·685	0·625	0·564	0·520	0·423
LOWER SURFACE	0·5	0·972	0·957	0·959	0·957	0·946	0·937	0·921	0·888	0·868
	1·5	0·941	0·917	0·918	0·915	0·901	0·892	0·874	0·840	0·820
	3	0·908	0·875	0·877	0·872	0·857	0·847	0·828	0·796	0·781
	6	0·881	0·837	0·837	0·832	0·816	0·806	0·786	0·756	0·736
	10	0·859	0·808	0·808	0·800	0·784	0·772	0·752	0·723	0·703
	18	0·832	0·771	0·770	0·763	0·743	0·730	0·709	0·677	0·656
	26	0·815	0·746	0·745	0·736	0·715	0·702	0·677	0·644	0·620
	34	0·802	0·726	0·724	0·713	0·689	0·676	0·648	0·615	0·588
	42	0·796	0·718	0·716	0·706	0·681	0·666	0·639	0·600	0·573
	50	0·790	0·708	0·706	0·696	0·670	0·654	0·624	0·582	0·552
	58	0·784	0·699	0·698	0·687	0·661	0·643	0·611	0·567	0·535
	66	0·780	0·694	0·692	0·681	0·651	0·634	0·600	0·546	0·509
	73	0·782	0·695	0·694	0·681	0·653	0·634	0·599	0·542	0·492
	79	0·780	0·694	0·692	0·681	0·652	0·630	0·593	0·536	0·485
	85	0·781	0·695	0·695	0·683	0·655	0·630	0·591	0·529	0·467
	91	0·785	0·701	0·700	0·690	0·664	0·633	0·591	0·530	0·462
	97	0·790	0·708	0·708	0·698	0·671	0·633	0·586	—	—
	100	0·796	0·713	0·726	0·715	0·685	0·625	0·564	0·520	0·423

TABLE 4

$\alpha = 5$ deg

Experimental Results : Detailed Pressure Distributions for 4 per cent thick Biconvex Aerofoil

	Hole position x/c (per cent)	Values of p/H_0								
		$M_0 =$ 0·70	$M_0 =$ 0·719	$M_0 =$ 0·732	$M_0 =$ 0·760	$M_0 =$ 0·780	$M_0 =$ 0·789	$M_0 =$ 0·809	$M_0 =$ 0·830	$M_0 =$ 0·848
UPPER SURFACE	1	0·444	0·408	0·106	0·090	0·095	0·105	0·139	0·157	0·176
	2	0·450	0·413	0·103	0·124	0·137	0·164	0·186	0·215	0·230
	5	0·448	0·411	0·200	0·217	0·224	0·242	0·261	0·287	0·298
	10	0·442	0·406	0·261	0·270	0·275	0·288	0·302	0·322	0·332
	16	0·450	0·421	0·293	0·296	0·299	0·310	0·321	0·340	0·348
	22	0·466	0·444	0·417	0·302	0·303	0·312	0·322	0·337	0·344
	28	0·492	0·472	0·509	0·310	0·308	0·317	0·325	0·338	0·343
	34	0·520	0·502	0·538	0·431	0·307	0·314	0·321	0·332	0·337
	40	0·547	0·528	0·573	0·499	0·312	0·318	0·327	0·335	0·337
	46	0·574	0·555	0·594	0·533	0·400	0·308	0·313	0·321	0·324
	52	0·597	0·580	0·609	0·556	0·489	0·462	0·311	0·317	0·319
	58	0·618	0·600	0·614	0·581	0·511	0·481	0·301	0·312	0·318
	64	0·643	0·619	0·621	0·595	0·524	0·494	0·438	0·305	0·310
	70	0·651	0·645	0·625	0·597	0·527	0·499	0·471	0·315	0·315
	76	0·664	0·648	0·637	0·605	0·540	0·503	0·474	0·312	0·311
	82	0·675	0·660	0·649	0·616	0·573	0·514	0·487	0·306	0·312
	88	0·684	0·669	0·664	0·634	0·607	0·523	0·494	0·311	0·311
	94	0·691	0·680	0·682	0·653	0·631	0·537	0·503	0·431	0·301
	97	0·699	0·685	0·696	0·667	0·631	0·541	0·509	0·458	0·330
	100	0·700	0·686	0·704	0·679	0·649	0·541	0·508	0·474	0·411
LOWER SURFACE	0·5	0·968	0·966	0·969	0·958	0·951	0·942	0·929	0·913	0·899
	1·5	0·931	0·928	0·930	0·917	0·908	0·898	0·883	0·866	0·851
	3	0·891	0·886	0·888	0·873	0·863	0·852	0·836	0·818	0·804
	6	0·854	0·848	0·848	0·831	0·821	0·809	0·793	0·774	0·760
	10	0·825	0·819	0·817	0·798	0·788	0·775	0·758	0·738	0·723
	18	0·789	0·781	0·777	0·756	0·745	0·730	0·713	0·691	0·675
	26	0·764	0·755	0·750	0·727	0·714	0·698	0·679	0·655	0·638
	34	0·745	0·734	0·727	0·700	0·687	0·667	0·645	0·618	0·600
	42	0·735	0·724	0·717	0·691	0·676	0·658	0·636	0·609	0·589
	50	0·724	0·713	0·706	0·678	0·662	0·643	0·619	0·589	0·568
	58	0·715	0·712	0·695	0·666	0·649	0·628	0·603	0·570	0·547
	66	0·707	0·696	0·687	0·656	0·638	0·615	0·587	0·548	0·520
	73	0·707	0·693	0·688	0·656	0·637	0·612	0·584	0·544	0·518
	79	0·702	0·689	0·684	0·653	0·633	0·602	0·573	0·530	0·505
	85	0·701	0·688	0·685	0·654	0·632	0·597	0·567	0·520	0·488
	91	0·702	0·689	0·690	0·661	0·635	0·591	0·561	0·515	0·476
	97	0·705	0·692	0·699	0·671	0·638	0·587	0·548	0·507	0·468
	100	0·700	0·686	0·704	0·679	0·649	0·541	0·508	0·474	0·411

TABLE 5

$\alpha = 6$ deg

Experimental Results : Detailed Pressure Distributions for 4 per cent thick Biconvex Aerofoil

	Hole position x/c (per cent)	Values of p/H_0								
		$M_0 =$ 0·60	$M_0 =$ 0·70	$M_0 =$ 0·737	$M_0 =$ 0·741	$M_0 =$ 0·746	$M_0 =$ 0·769	$M_0 =$ 0·779	$M_0 =$ 0·800	$M_0 =$ 0·834
UPPER SURFACE	1	0·595	0·473	0·384	0·076	0·083	0·083	0·088	0·093	0·118
	2	0·597	0·480	0·396	0·085	0·087	0·104	0·123	0·157	0·195
	5	0·595	0·479	0·396	0·180	0·183	0·197	0·209	0·227	0·259
	10	0·591	0·471	0·383	0·240	0·242	0·250	0·259	0·275	0·303
	16	0·588	0·472	0·402	0·281	0·267	0·275	0·281	0·294	0·318
	22	0·589	0·474	0·419	0·323	0·275	0·281	0·286	0·300	0·319
	28	0·602	0·491	0·441	0·455	0·430	0·288	0·292	0·305	0·322
	34	0·616	0·506	0·464	0·491	0·480	0·301	0·291	0·301	0·315
	40	0·635	0·526	0·483	0·501	0·492	0·461	0·394	0·306	0·318
	46	0·654	0·543	0·503	0·549	0·533	0·485	0·459	0·296	0·306
	52	0·669	0·561	0·523	0·567	0·555	0·497	0·481	0·295	0·304
	58	0·688	0·578	0·539	0·587	0·576	0·523	0·482	0·301	0·295
	64	0·703	0·595	0·556	0·600	0·593	0·544	0·491	0·447	0·289
	70	0·717	0·611	0·574	0·603	0·598	0·570	0·492	0·463	0·302
	76	0·729	0·626	0·588	0·614	0·610	0·585	0·501	0·456	0·297
	82	0·738	0·637	0·601	0·627	0·621	0·598	0·512	0·471	0·288
	88	0·747	0·648	0·612	0·642	0·638	0·614	0·519	0·476	0·296
	94	0·755	0·660	0·624	0·658	0·653	0·630	0·529	0·481	0·288
	97	0·758	0·665	0·630	0·670	0·665	0·639	0·534	0·489	0·340
	100	0·758	0·667	0·631	0·673	0·669	0·645	0·539	0·499	0·404
LOWER SURFACE	0·5	0·986	0·973	0·969	0·975	0·973	0·964	0·959	0·945	0·919
	1·5	0·957	0·937	0·930	0·926	0·935	0·923	0·916	0·883	0·859
	3	0·926	0·898	0·888	0·894	0·891	0·879	0·871	0·855	0·827
	6	0·897	0·861	0·848	0·853	0·851	0·836	0·828	0·810	0·781
	10	0·874	0·831	0·816	0·821	0·817	0·802	0·793	0·775	0·746
	18	0·845	0·794	0·775	0·775	0·776	0·758	0·748	0·728	0·697
	26	0·825	0·768	0·746	0·749	0·746	0·728	0·715	0·694	0·659
	34	0·810	0·747	0·722	0·725	0·720	0·699	0·685	0·653	0·619
	42	0·801	0·735	0·710	0·713	0·709	0·687	0·673	0·649	0·610
	50	0·793	0·723	0·696	0·700	0·695	0·671	0·656	0·631	0·590
	58	0·785	0·712	0·683	0·689	0·682	0·657	0·640	0·615	0·570
	66	0·778	0·702	0·672	0·677	0·671	0·645	0·626	0·596	0·543
	73	0·777	0·700	0·669	0·676	0·670	0·642	0·619	0·589	0·537
	79	0·773	0·693	0·660	0·671	0·663	0·636	0·609	0·578	0·523
	85	0·771	0·689	0·656	0·667	0·662	0·634	0·602	0·568	0·502
	91	0·770	0·686	0·653	0·674	0·662	0·637	0·592	0·559	0·495
	97	0·768	0·682	0·649	0·670	0·670	0·646	0·574	—	—
	100	0·758	0·667	0·631	0·673	0·669	0·645	0·539	0·499	0·404

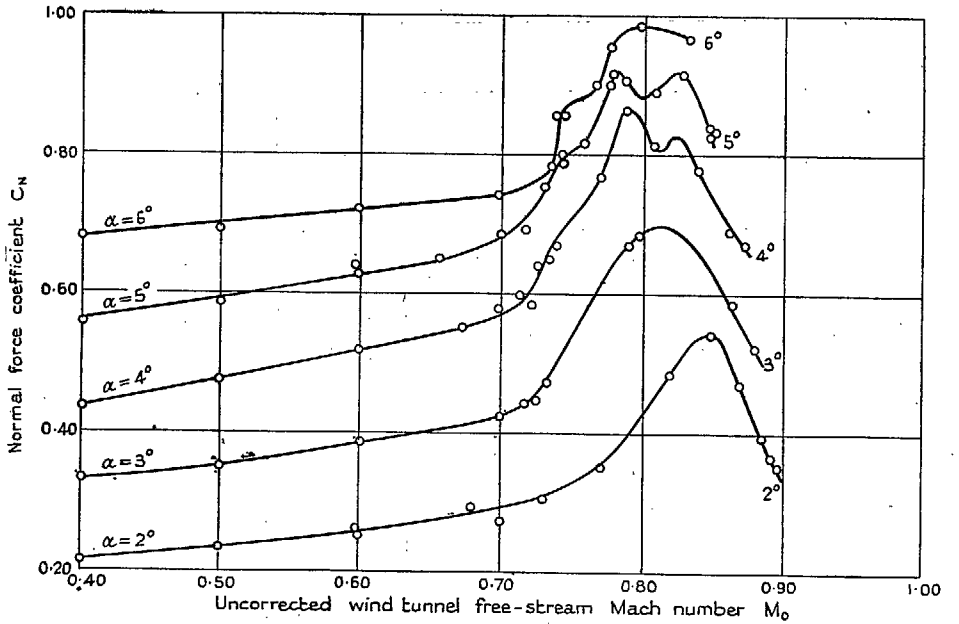

FIG. 1. Variation of normal-force coefficient with Mach number for 4 per cent thick biconvex aerofoil.

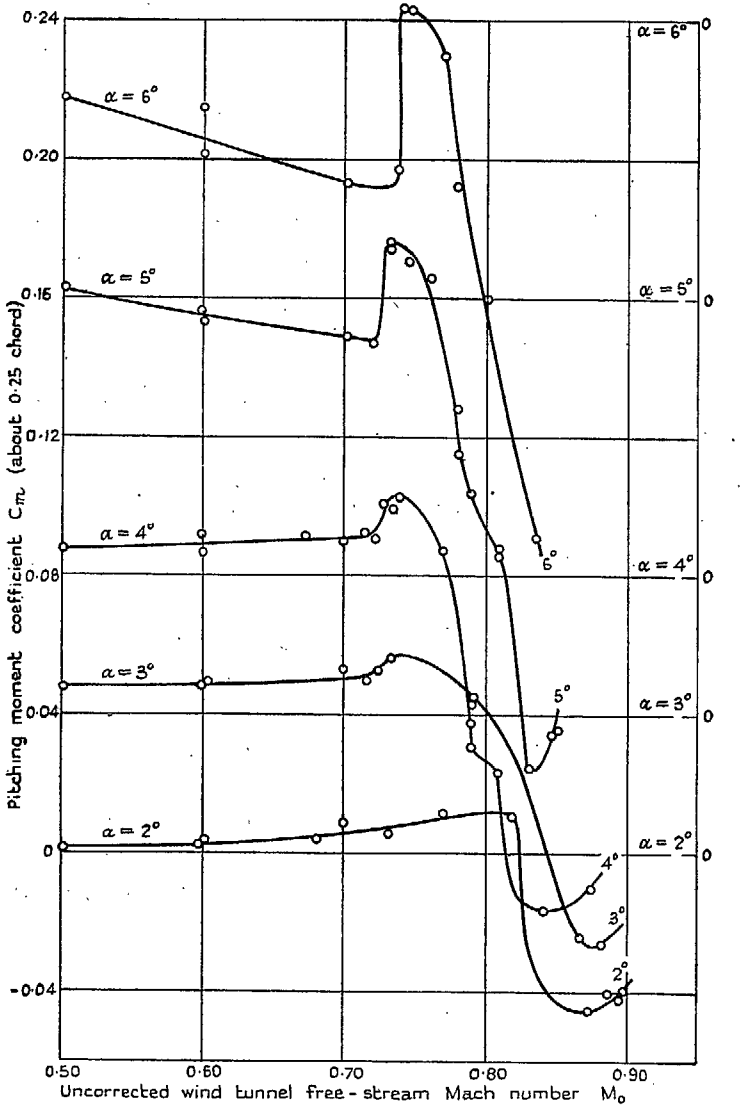

FIG. 2. Variation of pitching-moment coefficient with Mach number for 4 per cent thick biconvex aerofoil.

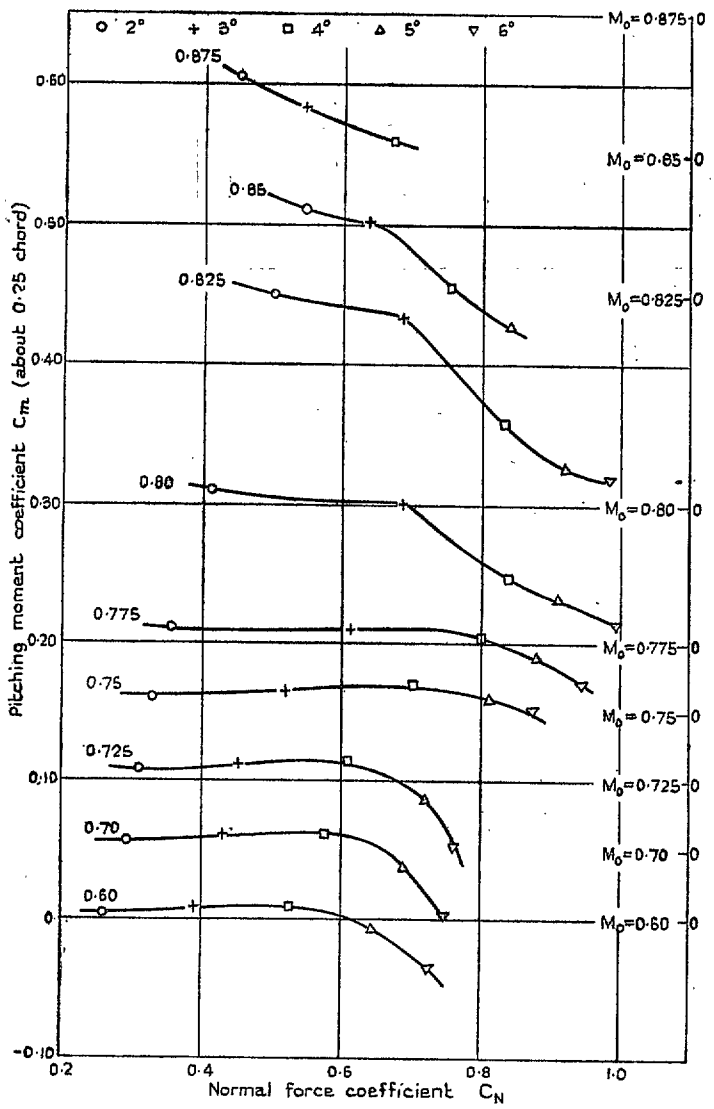

FIG. 3. Variation of pitching-moment coefficient with normal-force coefficient for a 4 per cent thick biconvex aerofoil.

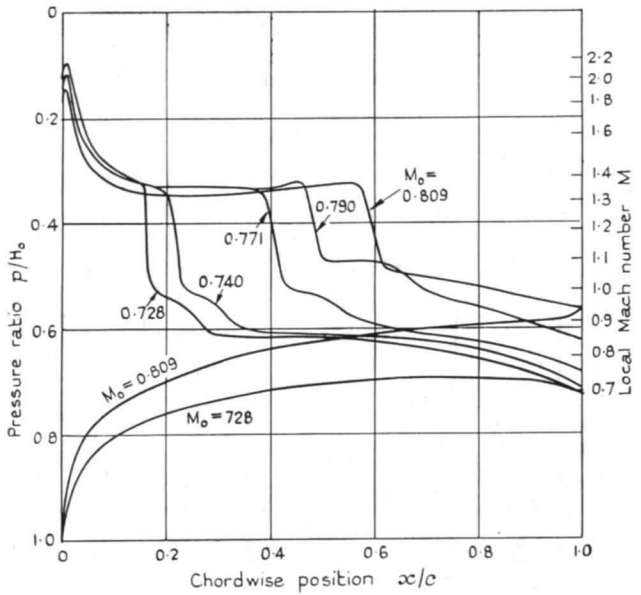

FIG. 4. Pressure distributions for a 4 per cent thick biconvex aerofoil at $\alpha = 4$ deg.

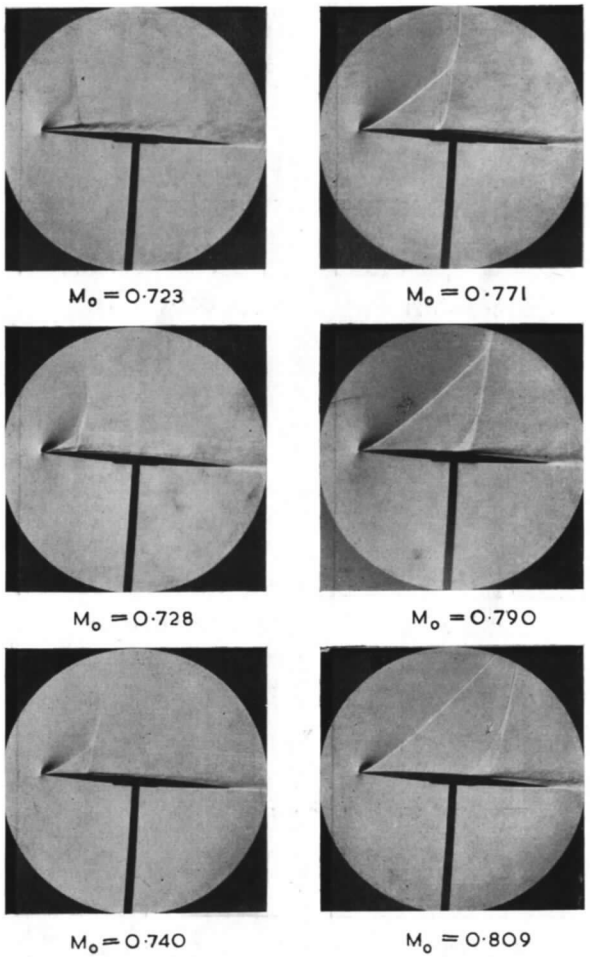

FIG. 5. Schlieren photographs of the flow past a 4 per cent thick biconvex aerofoil at an incidence of 4 deg.

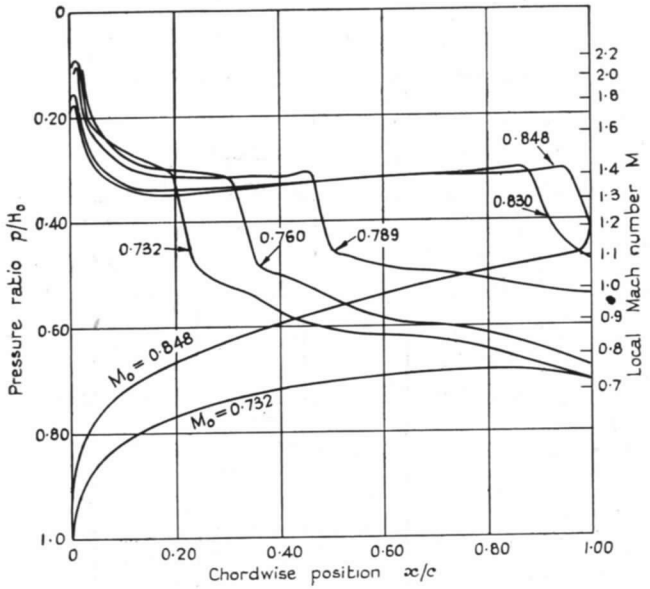

FIG. 6. Pressure distributions for a 4 per cent thick biconvex aerofoil at $\alpha = 5$ deg.

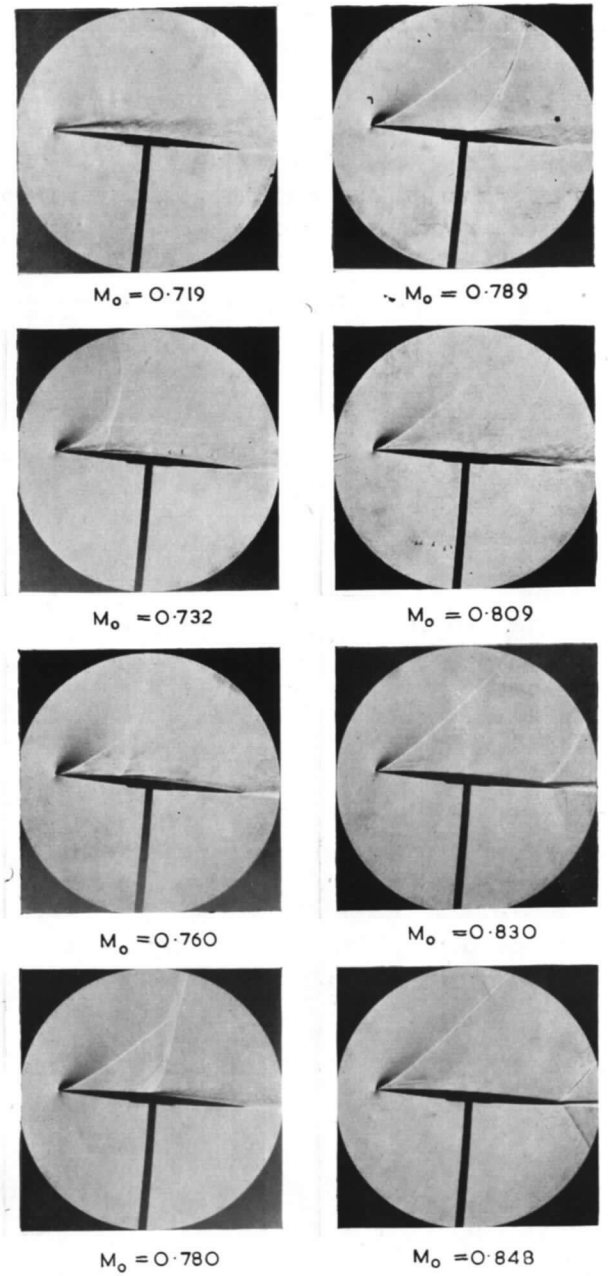

FIG. 7. Schlieren photographs of the flow past a 4 per cent thick biconvex aerofoil at an incidence of 5 deg.

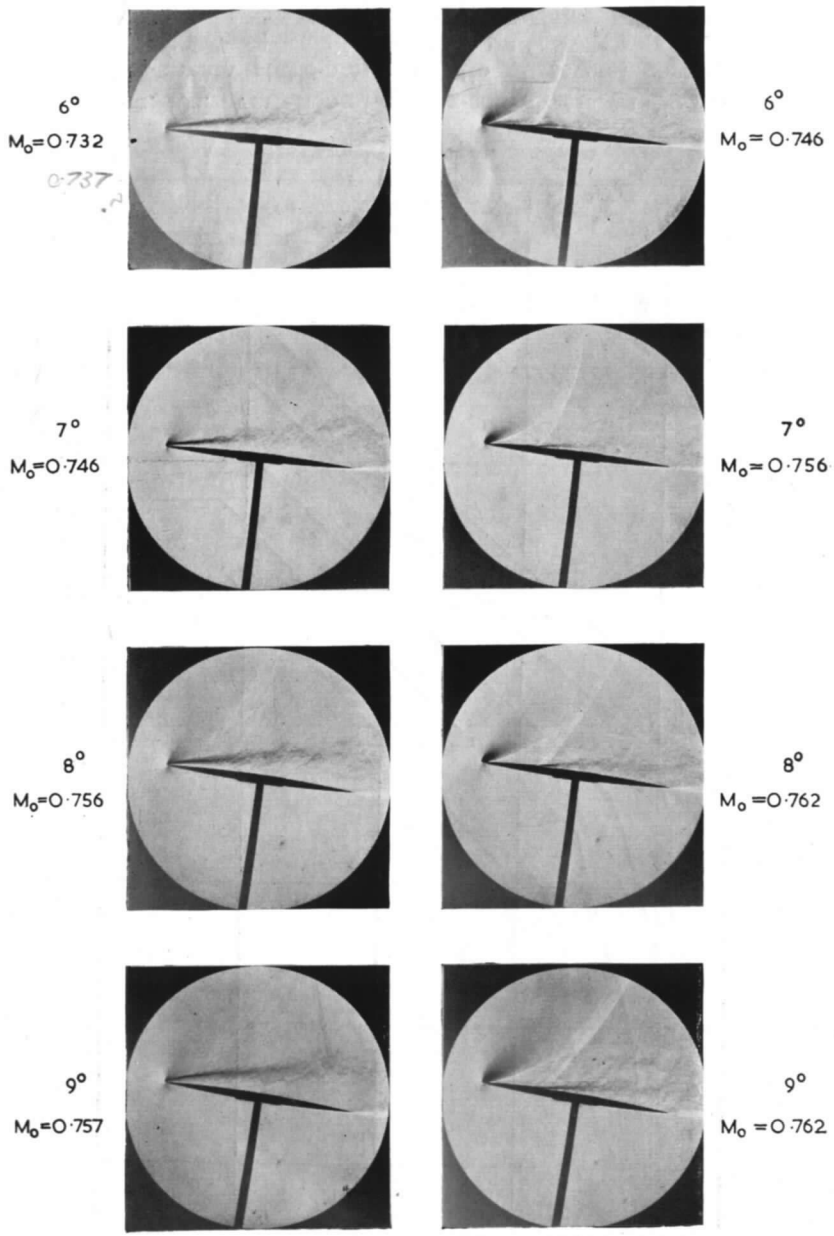

FIG. 8. Schlieren photographs of the change from leading-edge to shock-induced separation for a 4 per cent thick biconvex aerofoil.

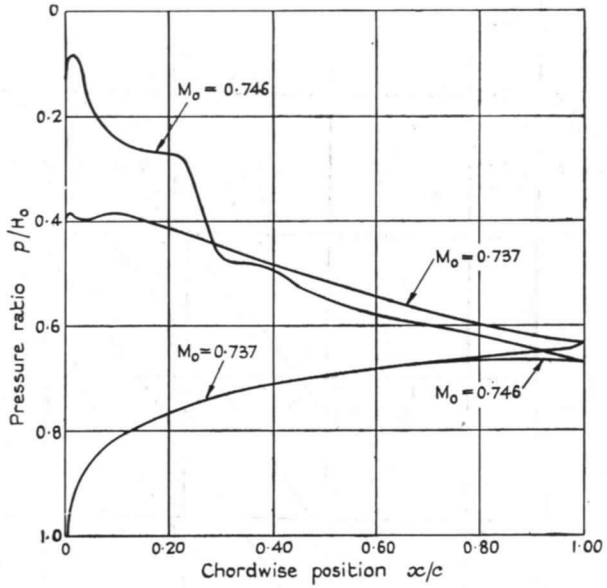

FIG. 9. Pressure distributions for a 4 per cent thick biconvex aerofoil at $\alpha = 6$ deg, showing the change from leading-edge to shock-induced separation.

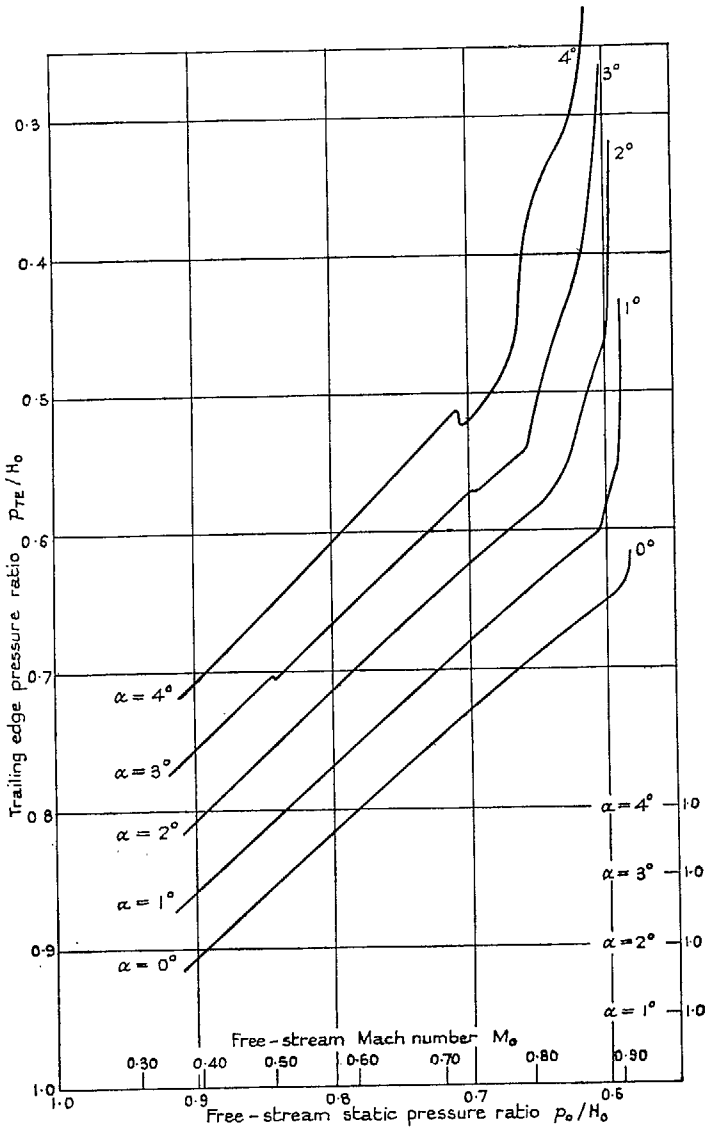

FIG. 10a. Variation of trailing-edge pressure ratio with free-stream static-pressure ratio at several constant incidences for a 4 per cent thick biconvex aerofoil.

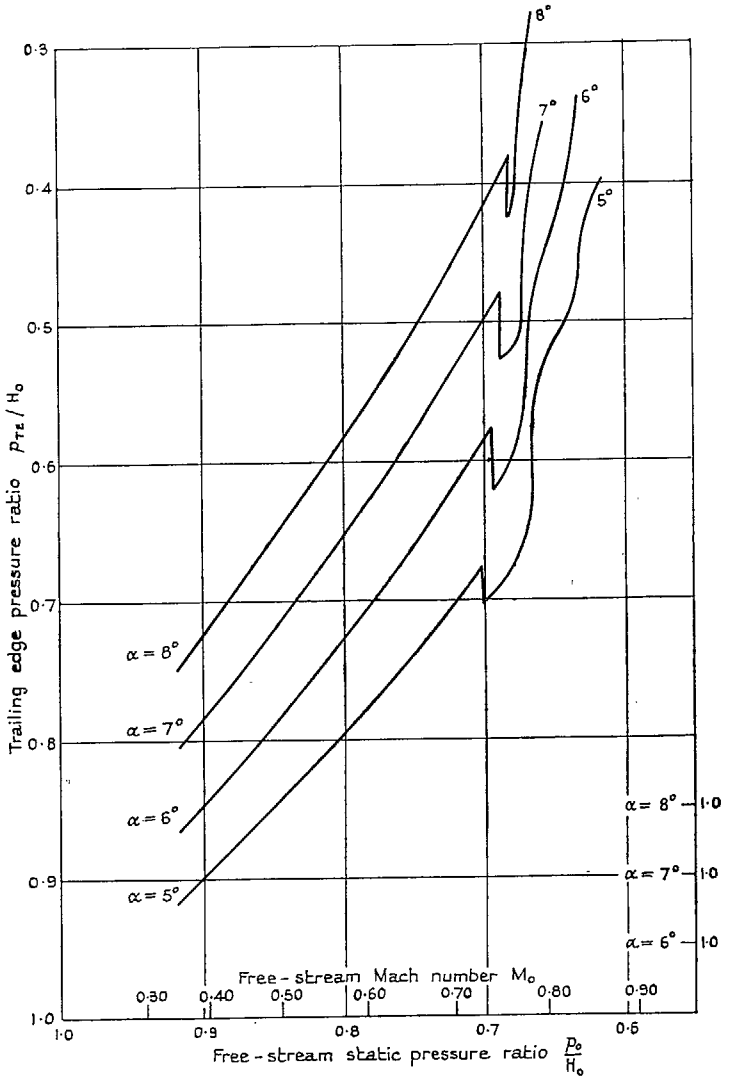

FIG. 10b. Variation of trailing-edge pressure ratio with free-stream static-pressure ratio at several constant incidences for a 4 per cent thick biconvex aerofoil.

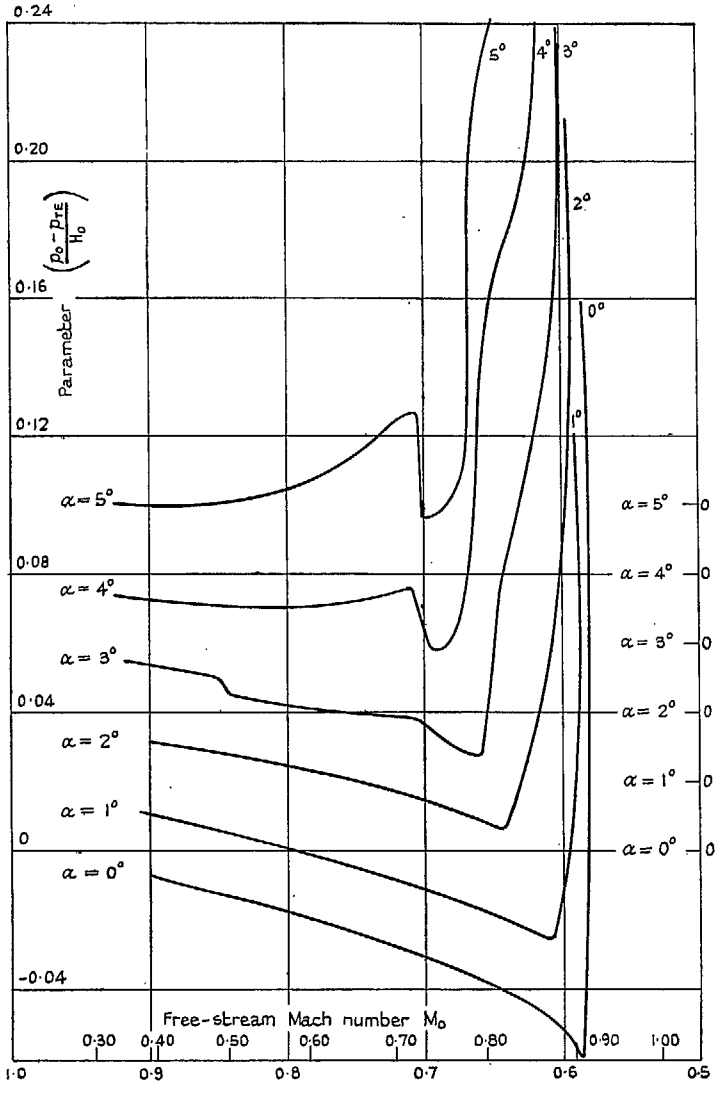

FIG. 11a. Variation of parameter $(p_0 - p_{TE})/H_0$ with free-stream static-pressure ratio at several constant incidences for a 4 per cent thick biconvex aerofoil.

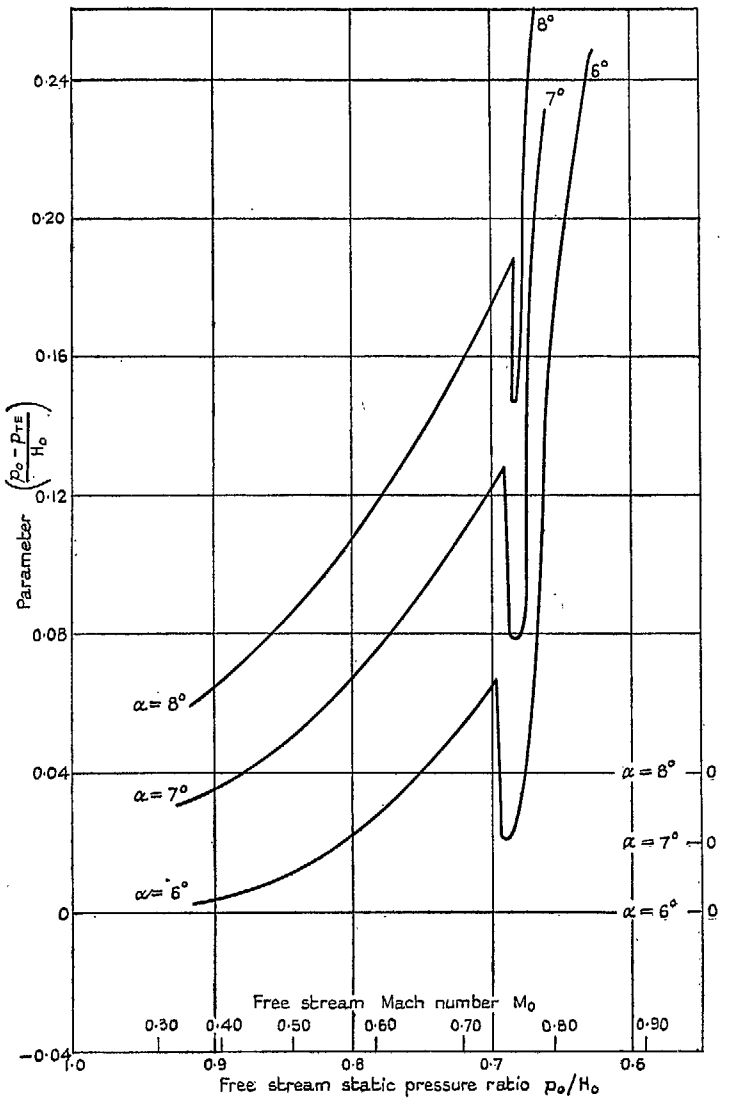

FIG. 11b. Variation of parameter $(p_0 - p_{TE})/H_0$ with free-stream static-pressure ratio at several constant incidences for a 4 per cent thick biconvex aerofoil.

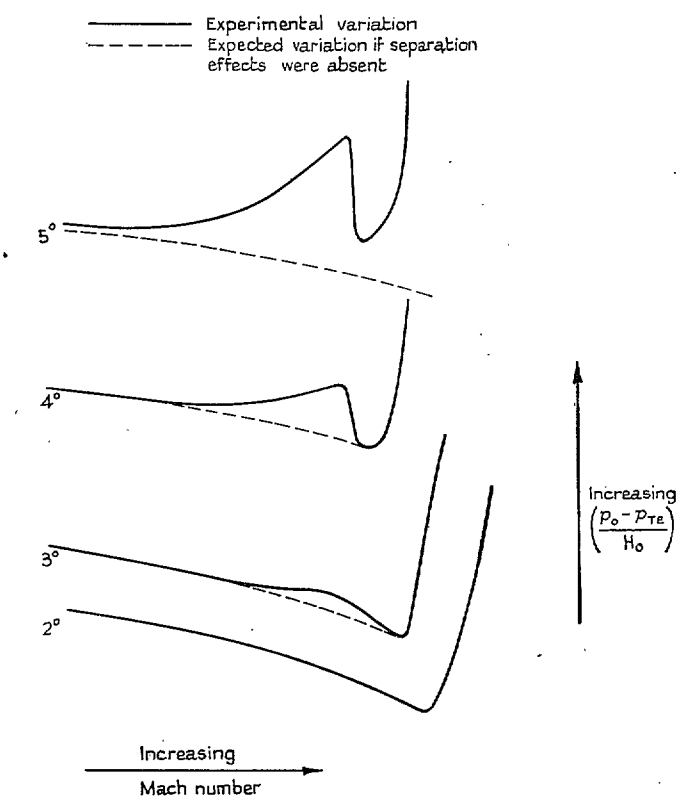

FIG. 11c. Schematic variation of parameter $(p_0 - p_{TE})/H_0$ with free-stream Mach number at several constant incidences for a 4 per cent thick biconvex aerofoil.

(73171) Wt. 53/2293 K.7 8/58 Hw.

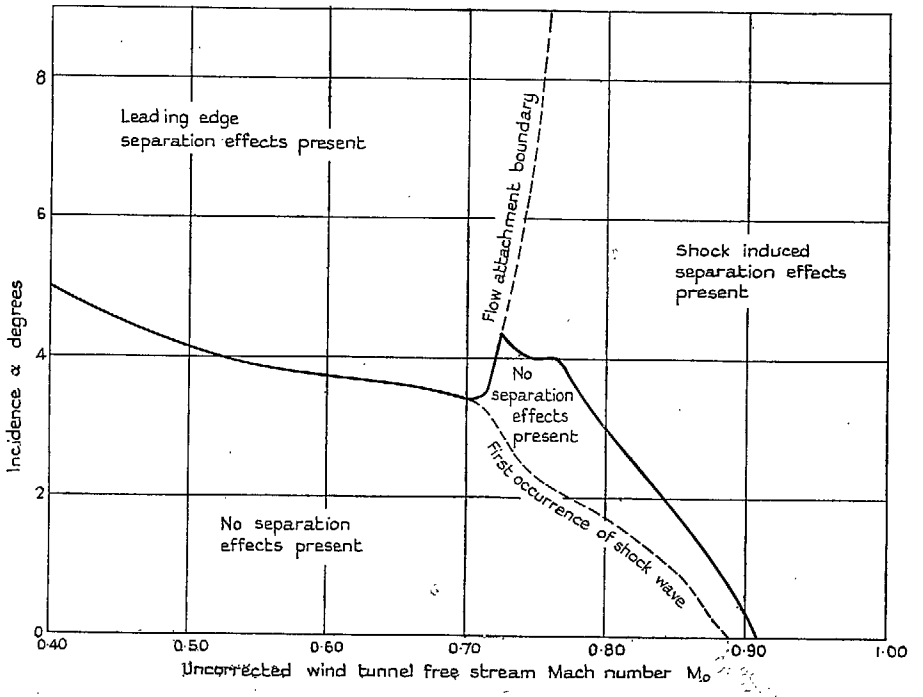

FIG. 12. Divergence boundary for a two-dimensional 4 per cent thick biconvex aerofoil at subsonic speeds.

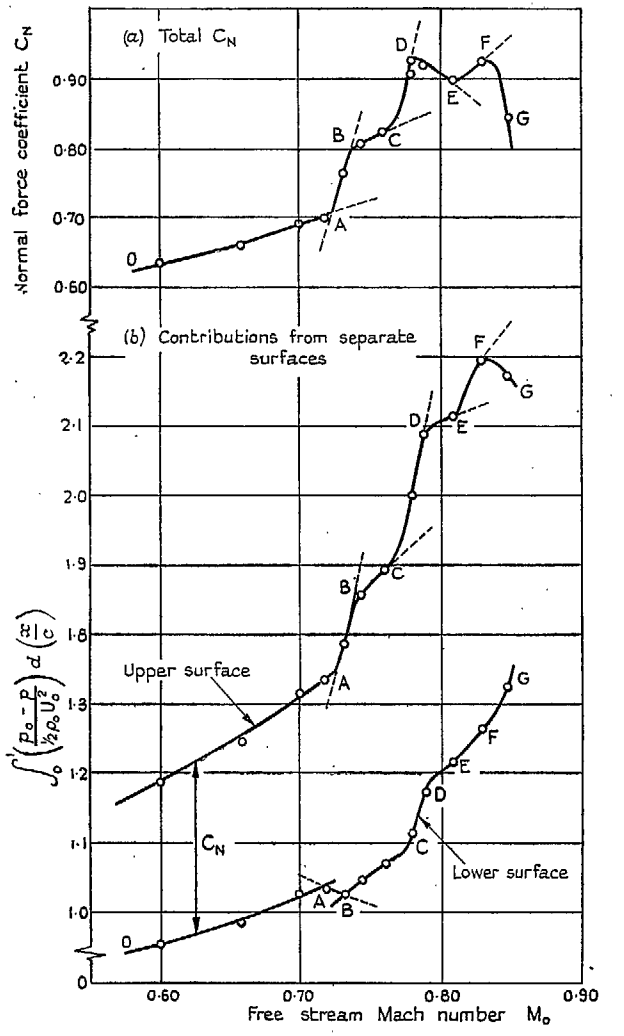

FIG. 13. Observations for a 4 per cent thick biconvex aerofoil at 5 deg incidence. Variation of the total C_N and the contributions from the separate surfaces with free-stream Mach number.

PRINTED IN GREAT BRITAIN

Publications of the Aeronautical Research Council

ANNUAL TECHNICAL REPORTS OF THE AERONAUTICAL RESEARCH COUNCIL (BOUND VOLUMES)

1939 Vol. I. Aerodynamics General, Performance, Airscrews, Engines. 50*s.* (52*s.*).
Vol. II. Stability and Control, Flutter and Vibration, Instruments, Structures, Seaplanes, etc. 63*s.* (65*s.*)

1940 Aero and Hydrodynamics, Aerofoils, Airscrews, Engines, Flutter, Icing, Stability and Control, Structures, and a miscellaneous section. 50*s.* (52*s.*)

1941 Aero and Hydrodynamics, Aerofoils, Airscrews, Engines, Flutter, Stability and Control, Structures. 63*s.* (65*s.*)

1942 Vol. I. Aero and Hydrodynamics, Aerofoils, Airscrews, Engines. 75*s.* (77*s.*)
Vol. II. Noise, Parachutes, Stability and Control, Structures, Vibration, Wind Tunnels. 47*s.* 6*d.* (49*s.* 6*d.*)

1943 Vol. I. Aerodynamics, Aerofoils, Airscrews. 80*s.* (82*s.*)
Vol. II. Engines, Flutter, Materials, Parachutes, Performance, Stability and Control, Structures. 90*s.* (92*s.* 9*d.*)

1944 Vol. I. Aero and Hydrodynamics, Aerofoils, Aircraft, Airscrews, Controls. 84*s.* (86*s.* 6*d.*)
Vol. II. Flutter and Vibration, Materials, Miscellaneous, Navigation, Parachutes, Performance, Plates and Panels, Stability, Structures, Test Equipment, Wind Tunnels. 84*s.* (86*s.* 6*d.*)

1945 Vol. I. Aero and Hydrodynamics, Aerofoils. 130*s.* (132*s.* 9*d.*)
Vol. II. Aircraft, Airscrews, Controls. 130*s.* (132*s.* 9*d.*)
Vol. III. Flutter and Vibration, Instruments, Miscellaneous, Parachutes, Plates and Panels, Propulsion. 130*s.* (132*s.* 6*d.*)
Vol. IV. Stability, Structures, Wind Tunnels, Wind Tunnel Technique. 130*s.* (132*s.* 6*d.*)

Annual Reports of the Aeronautical Research Council—

1937 2*s.* (2*s.* 2*d.*) 1938 1*s.* 6*d.* (1*s.* 8*d.*) 1939–48 3*s.* (3*s.* 5*d.*)

Index to all Reports and Memoranda published in the Annual Technical Reports, and separately—

April, 1950 - - - - R. & M. 2600 2*s.* 6*d.* (2*s.* 10*d.*)

Author Index to all Reports and Memoranda of the Aeronautical Research Council—

1909—January, 1954 R. & M. No. 2570 15*s.* (15*s.* 8*d.*)

Indexes to the Technical Reports of the Aeronautical Research Council—

December 1, 1936—June 30, 1939	R. & M. No. 1850	1*s.* 3*d.* (1*s.* 5*d.*)
July 1, 1939—June 30, 1945	R. & M. No. 1950	1*s.* (1*s.* 2*d.*)
July 1, 1945—June 30, 1946	R. & M. No. 2050	1*s.* (1*s.* 2*d.*)
July 1, 1946—December 31, 1946	R. & M. No. 2150	1*s.* 3*d.* (1*s.* 5*d.*)
January 1, 1947—June 30, 1947	R. & M. No. 2250	1*s.* 3*d.* (1*s.* 5*d.*)

Published Reports and Memoranda of the Aeronautical Research Council—

Between Nos. 2251–2349	R. & M. No. 2350	1*s.* 9*d.* (1*s.* 11*d.*)
Between Nos. 2351–2449	R. & M. No. 2450	2*s.* (2*s.* 2*d.*)
Between Nos. 2451–2549	R. & M. No. 2550	2*s.* 6*d.* (2*s.* 10*d.*)
Between Nos. 2551–2649	R. & M. No. 2650	2*s.* 6*d.* (2*s.* 10*d.*)
Between Nos. 2651–2749	R. & M. No. 2750	2*s.* 6*d.* (2*s.* 10*d.*)

Prices in brackets include postage

HER MAJESTY'S STATIONERY OFFICE

York House, Kingsway, London W.C.2; 423 Oxford Street, London W.1; 13a Castle Street, Edinburgh 2; 39 King Street, Manchester 2; 2 Edmund Street, Birmingham 3; 109 St. Mary Street, Cardiff; Tower Lane, Bristol 1; 80 Chichester Street, Belfast, *or through any bookseller.*

S.O. Code No. 23-3092